Realistic Modeling of Multi-Scale MHD Dynamics of the Solar Atmosphere

Irina Kitiashvili[1], Nagi N. Mansour[1], Alan Wray[1], Sebastien Couvidat[2], Seokkwan Yoon[1], Alexander Kosovichev[1,3]

[1]NASA Ames Research Center, [2]Stanford University, [3]New Jersey Institute of Technology

Realistic 3D radiative MHD simulations open new perspectives for understanding the turbulent dynamics of the solar surface, its coupling to the atmosphere, and the physical mechanisms of generation and transport of non-thermal energy. Traditionally, plasma eruptions and wave phenomena in the solar atmosphere are modeled by prescribing artificial driving mechanisms using magnetic or gas pressure forces that might arise from magnetic field emergence or reconnection instabilities. In contrast, our 'ab initio' simulations provide a realistic description of solar dynamics naturally driven by solar energy flow. By simulating the upper convection zone and the solar atmosphere, we can investigate in detail the physical processes of turbulent magnetoconvection, generation and amplification of magnetic fields, excitation of MHD waves, and plasma eruptions. We present recent simulation results of the multi-scale dynamics of quiet-Sun regions, and energetic effects in the atmosphere and compare them with observations. For the comparisons we calculate synthetic spectro-polarimetric data to model observational data from *SDO*, *Hinode*, and the BBSO New Solar Telescope.

'SolarBox' code

- ✓ 3D rectangular geometry
- ✓ Fully conservative, Fully compressible
- ✓ Fully coupled radiation solver:
  - − LTE using 4 opacity-distribution-function bins
  - − Ray-tracing transport by Feautrier method
  - − 18 ray (2 vertical, 16 slanted) angular quadrature
- ✓ Non-ideal (tabular) EOS
- ✓ 4th order Padé spatial discretization
- ✓ 4th order Runge-Kutta time integration
- ✓ LES-Eddy Simulation options (turbulence models):
  - Compressible Smagorinsky model
  - Compressible Dynamics Smagorinsky mode (Germano et a., 1991; Moin et al, 1991)
  - MHD subgrid models (Balarac et al., 2010)
  - DNS+Hyperviscosity approach
- ✓ MPI parallelization (plane and pencil versions)

Basic equations

The equations are the grid-cell averaged

Conservation of mass: $$\frac{\partial \rho}{\partial t} + \left(\rho u_i\right)_{,i} = 0$$

Conservation of momentum: $$\frac{\partial \rho u_i}{\partial t} + \left(\rho u_i u_j + P_{ij}\right)_{,j} = -\rho\phi_{,i}$$

Conservation of energy:

$$\frac{\partial E}{\partial t} + \left(\begin{array}{l} Eu_i + P_{ij}u_j - \kappa T_{,i} + \\ + \left(\frac{c}{4\pi}\right)^2 \frac{1}{\sigma}\left(B_{i,j} - B_{j,i}\right)B_j + F_i^{\mathrm{rad}} \end{array} \right)_{,i} = 0$$

with

$$P_{ij} = \left(p + \frac{2}{3}\mu u_{k,k} + \frac{1}{8\pi}B_k B_k\right)\delta_{ij} - \mu\left(u_{i,j} + u_{j,i}\right) - \frac{1}{4\pi}B_i B_j$$

Conservation of magnetic flux

$$\frac{\partial B_i}{\partial t} + \left(u_j B_i - u_i B_j - \frac{c^2}{4\pi\sigma}\left(B_{i,j} - B_{j,i}\right)\right)_{,j} = 0$$

'SolarBox' code

1) 80 x 80 x 26 Mm
2) 6.4 x 6.4 x 6 Mm

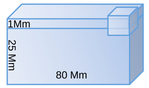

Initial magnetic field:

0 G
10^{-6}-10^{-2} G
10 G
100 G

SPINOR code

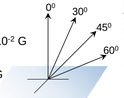

Magnetized vortex tubes and flow eruptions

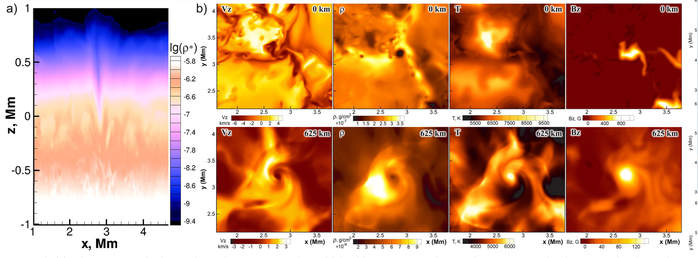

Panel (a) shows a vertical cut through a vortex tube which drives an eruption and generates shock waves in the solar chromosphere. Horizontal cuts (panel (b) show a fraction of the domain at the photosphere (top row) and at 625 km above the solar surface (bottom row) for different quantities (left to right): vertical velocity, density, temperature, and vertical magnetic field.

$$\frac{\partial \mathbf{v}}{\partial t} + (\mathbf{v}\cdot\nabla)\mathbf{v} = \boxed{\frac{\mathbf{J}\times\mathbf{B}}{c\rho}} - \boxed{\frac{\nabla p}{\rho}} - g$$

Comparison of the contributions to the flow ejection of the hydrodynamic (red curves) and magnetic (Lorentz force, blue curves) vertical accelerations (normalized by the gravity acceleration) at different altitudes: (a) h = 780 km, (b) h = 300 km, (c) h = 0 km (photosphere), and (d) h = −240 km. The dashed curves correspond to the vertical velocity, V_z, given for reference at the same layers.

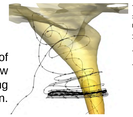

Structure of the flow during eruption.

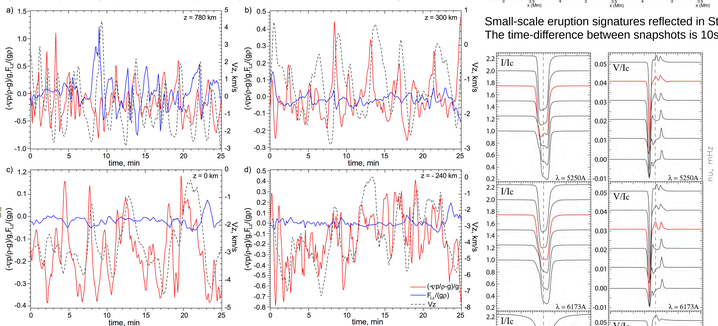

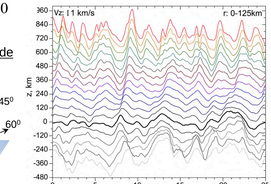

Temporal profiles of variations of the mean vertical velocity at different levels below the surface and in the atmosphere. The thick black curve shows the variations in the photosphere layer. The height difference between the curves is 60 km.

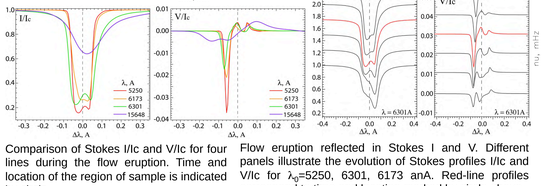

Comparison of Stokes I/Ic and V/Ic for four lines during the flow eruption. Time and location of the region of sample is indicated by circle.

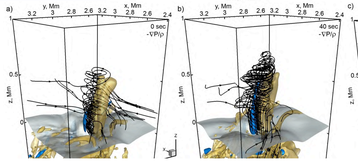

Different stages of a flow ejection. Black streamlines illustrate the velocity field in the vicinity of a vortex tube. Semitransparent light gray surface corresponds to a constant temperature of 6400 K. Yellow and blue isosurfaces show the vertical pressure gradient divided by density ($-\nabla p/\rho$) is equal to $5\cdot10^4$ cm/s^2 (yellow color) and $-5\cdot10^4$ cm/s^2 (blue color).

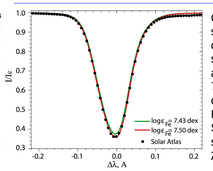

Comparison of the synthetic line profiles obtained from our simulations for two iron abundances: 7.43 and 7.50 dex, and from observations with Fourier Transform Spectrometer (FTS solar atlas) for the line λ_0 = 6173.3 A.

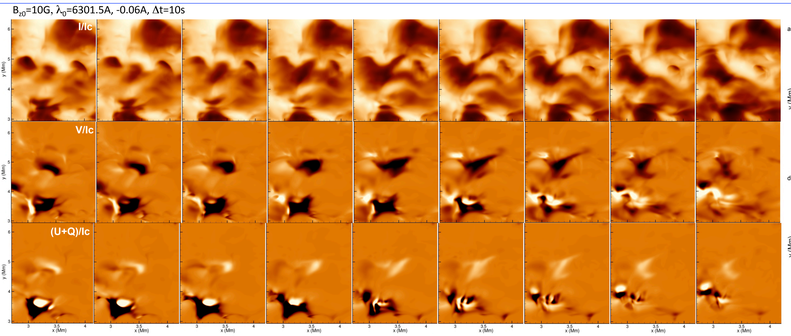

Small-scale eruption signatures reflected in Stokes I, V and (U+Q). Panels show zoomed images of I/Ic, V/Ic and (U+Q)/Ic for λ$_0$=−0.06A (λ$_0$=6301.5A). The time-difference between snapshots is 10s. White circle shows the location of a probe for studying the evolution of the Stokes profile shape.

Flow eruption reflected in Stokes I and V. Different panels illustrate the evolution of Stokes profiles I/Ic and V/Ic for λ_0=5250, 6301, 6173 anA. Red-line profiles correspond to time and location marked by circle above.

Modeling center-to-limb variations of the HMI observables

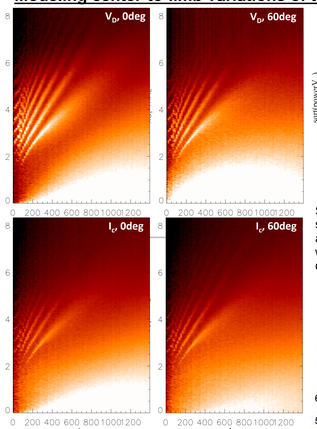

Ridges in nu, *l* - plane calculated from the synthetic data (Fe I, 6173A): Doppler shift (top) and continuum intensity (bottom) for 0^0 and 60^0 from the solar disk center.

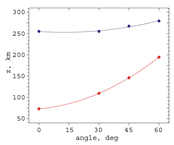

Variation of the height of formation of the 6173.3 A line as a function of the angular distance from the solar disc center for the full-resolution (red dots) and HMI resolution (blue). Both sets of data are fit with a second order polynomial.

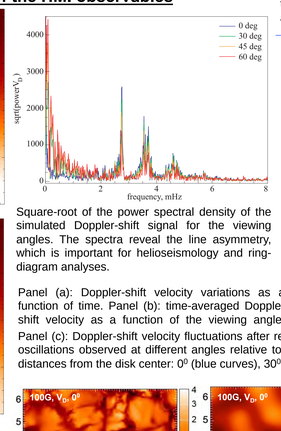

Square-root of the power spectral density of the simulated Doppler-shift signal for the viewing angles. The spectra reveal the line asymmetry, which is important for helioseismology and ring-diagram analyses.

Panel (a): Doppler-shift velocity variations as a function of time. Panel (b): time-averaged Doppler shift velocity as a function of the viewing angle.

Panel (c): Doppler-shift velocity fluctuations after removing the angular dependence. Panel (d): cross-correlations of the oscillations observed at different angles relative to the disk center. Different line colors correspond to different angular distances from the disk center: 0^0 (blue curves), 30^0 (green), 45^0 (orange) and 60^0 (red curves).

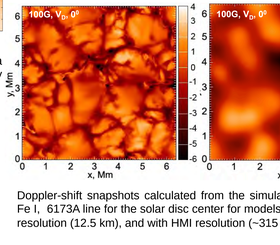

Doppler-shift snapshots calculated from the simulated profiles of the Fe I, 6173A line for the solar disc center for models with full numerical resolution (12.5 km), and with HMI resolution (~315 km/pixel).

Local dynamo simulations

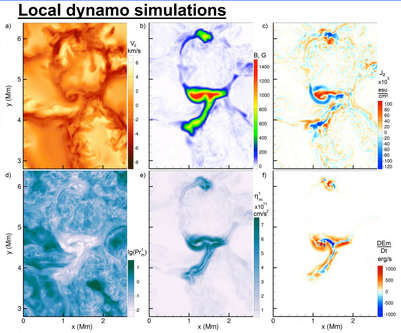

Horizontal snapshot of a fraction of the computational domain in the photosphere for: a) the vertical velocity; b) magnetic field strength; c) vertical component of the electric current density; d) logarithm of the turbulent magnetic Prandtl number; e) turbulent magnetic diffusivity; and f) time-derivative of the magnetic energy density.

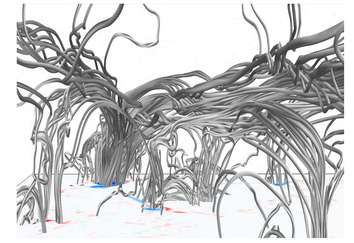

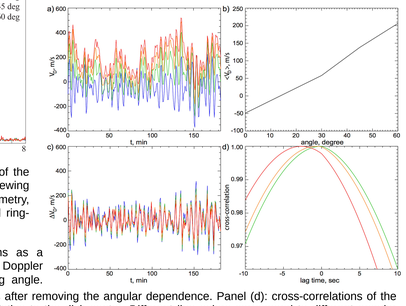

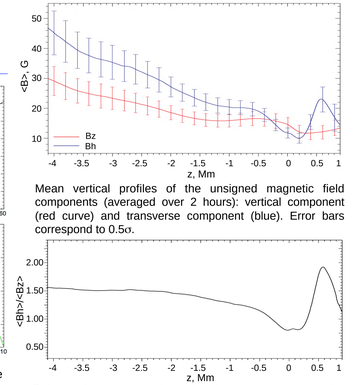

Conclusions

Realistic 3D radiative hydrodynamic simulations allow us to investigate important links between solar observations and the physical and dynamical properties of solar conditions. This is achieved by taking into account spectral line formation conditions, line-of-sight effects, and instrumental spatial and spectral resolutions. It is important to model the observational and data analysis procedures and calculate `observables' using the simulation data to achieve direct comparison of observations and numerical models .

The small-scale dynamics are not easily observed in broad-band images even with high observational spatial resolution. We examine four lines (5250A, 6173A, 6301A and 15648A) for studying the temporal evolution of the Stokes profiles during small-scale flow eruptions in magnetic field regions. The synthetic Stokes profiles reveal interesting variations in the form of 'running-wave' perturbations across the line with time - reflecting the bidirectional flow dynamics of the eruptions. The Stokes images show ubiquitous small-scale elongated structures which originate in the photosphere. Some of these can be identified as ultrafine loops above the granulation.

We found that the primary topology of the dynamo-generated magnetic field is represented by compact magnetic loops appearing as bipolar structures in the intergranular lanes, where the height of the loops is greater for stronger magnetic field concentrations at the foot-points. The formation of magnetic loops in the solar atmosphere causes the observed anisotropy as a function of height of the vertical and transverse small-scale magnetic fields.